Journal of The Electrochemical Society, **159** (3) B355-B359 (2012)
0013-4651/2012/159(3)/B355/5/$28.00 © The Electrochemical Society

Chemical Selectivity during the Electro-Oxidation of Ethanol on Unsupported Pt Nanoparticles

Daniel A. Cantane* and Ernesto R. Gonzalez,z**

Instituto de Química de São Carlos, Universidade de São Paulo, CEP 13560-970, CP780 São Carlos-SP, Brazil

In this paper we present results on the electro-oxidation of ethanol on unsupported (carbon free) platinum nanoparticles, considering the effects of the alcohol concentration. The case of the so-called dual pathway mechanism during the electro-oxidation of ethanol showed to be influenced by the surface coverage of adsorbed carbon monoxide (CO_{ad}) at unsupported platinum. The influences of adsorbed intermediates were followed by *in situ* infrared spectroscopy (FTIR) and by electrochemical experiments. Unsupported platinum showed that the reaction leads to the formation of CO_2 and acetic acid as main products at low concentrations of ethanol (0.01 to 0.1 mol L^{-1}). At least in this case of 0.01 mol L^{-1} ethanol, most formation of CO_2 occurred *via* CO_{ad} (indirect pathway). At higher concentration of ethanol, however, most CO_2 was formed *via* a reactive intermediate such as acetaldehyde (direct pathway). In addition, in this higher concentration of ethanol, the acetic acid was produced *via* formation of adsorbed acetaldehyde (*via* acetate) at higher overpotentials. In case of the acetic acid formation, a dual pathway was identified during the electro-oxidation of ethanol at low alcohol concentrations, whereas a parallel pathway occurred without the formation of adsorbed acetate intermediates at low overpotentials.

Manuscript submitted June 9, 2011, revised manuscript received December 20, 2011. Published January 17, 2012. This was Paper 1011 presented at the Vienna, Austria, Meeting of the Society, October 4–9, 2009.

In large urban centers, the society is based on a model of living that contributes to a growing environmental disorder and damage. Therefore, it is necessary to develop renewable energy sources that contribute to progress and development with appropriate environmental preservation. Because of this, fuel cell systems have become a promising alternative[1–3] and, as renewable fuel of low toxicity and high power density, ethanol is a good candidate for these applications.[3] However, the electro-oxidation of ethanol catalyzed by platinum presents a complex reaction mechanism involving several steps, diminishing the efficiency of the fuel cell.[4,5] In order to understand better the mechanism during the electro-oxidation of ethanol, in situ spectroscopic techniques, such as Fourier Transform Infra-red (FTIR),[4–8] and vibrational Sum-Frequency Generation (SFG),[18] besides *on-line* Differential Electrochemical Mass Spectrometry (DEMS),[4,9,10] have been used by Vielstich,[12] Weaver,[13] Lenza,[8] Iwasita[4,6,14] and coworkers, as well as Behm group,[9,11,16] Koper group,[16,17,19] Wieckowski group,[18,20] Baltruschat group[25,26] and our group.[5,6,10,14,15,21–24] Due to these efforts, the molecular nature of intermediates and products of the electro-oxidation of ethanol are relatively well-known.

Likewise the case of most small organic molecules,[27] the electro-oxidation of ethanol occurs through the so-called dual pathway mechanism for CO_2 formation. The indirect pathway proceeds *via* the formation of adsorbed carbon monoxide (CO_{ad}),[4,6,9,26] formed from the dissociative adsorption of ethanol reacting with adsorbed oxygenated species to be oxidized to CO_2. In this case of indirect pathway, the formation of adsorbed hydrocarbon fragments may occur (CH_{ad} with one or two carbons) which are oxidized to CO_2 at higher overpotentials.[9,16,18,19,26] The direct pathway, at the same time, occurs *via* a reactive intermediate as acetaldehyde.[7,26,18] In parallel, the electro-oxidation of ethanol may form acetaldehyde and acetic acid as end-products of the reaction.[9,22,25,26]

Additionally, the dual pathway mechanism during the electro-oxidation of ethanol has been reported to be influenced by the concentration of alcohol,[6,7,22] which promotes different yields on the products. The effect of the alcohol concentration on the electro-oxidation of ethanol has not been studied at unsupported platinum nanostructures. Furthermore, the electro-oxidation of ethanol catalyzed by unsupported platinum is interesting because of i) the possibility of different electrocatalytic characteristics when compared with bulk and single crystal platinum[28,29] and ii) the use of unsupported platinum particles for the preparation of fuel cell electrodes has been described several times.[30,31]

In this paper we propose a reaction mechanism on the electro-oxidation of ethanol on unsupported Pt (J-M) agglomerates. We were able to show new insights for surface coverage of adsorbed carbon monoxide (CO_{ad}) during the electro-oxidation of ethanol on unsupported platinum, which is influenced by the alcohol concentration. In addition, our data showed that the formation of acetic acid as product occurs through a dual pathway, and proceeds without the formation of adsorbed acetate intermediate at least at low alcohol concentrations. The formation of products and the influences of adsorbed intermediates during the ethanol electro-oxidation on unsupported platinum nanoparticles were identified by in situ infrared spectroscopy (FTIR) and by electrochemical experiments.

Materials and Methods

Instrumentation.— The electrochemical cell was a conventional 3 compartment cell with a reversible hydrogen electrode (RHE) as reference and a high surface area Au electrode as auxiliary, both separated from the main compartment. All potentials in this work were referred to this reversible hydrogen electrode (RHE). Cyclic voltammetric and chronoamperometric measurements were recorded in the potentiostatic mode using a 1287A Solartron potentiostat.

In situ FTIR measurements were carried out using a Nexus 670 – Nicolet equipment equipped with a MCT detector and a ZnSe flat window. Details of the spectroelectrochemical cell are given elsewhere[14]. The reflectance spectra were obtained as R/Ro where R was the sample spectrum. The reference spectra (Ro) were recorded at 0.05 V or 1.0 V which were related to the band intensity at the detector and associated frequency of the species. This procedure results in spectra with negative and positive bands related to the production and the consumption of substances, respectively. Spectra were computed from an average of 64 interferograms. The spectral resolution was 8 cm^{-1}.

Electrodes, conditions, solutions.— Working electrode (WE) supports for the electrochemical and in situ FTIR experiments were polycrystalline Au disks with diameters 0.65 cm^2 and 1.0 cm^2, respectively. Both working electrodes were prepared in the form of a thin film by applying 20 μL of an aqueous suspension of the black platinum catalyst (16.7 mg mL^{-1}, Pt-JM - *Johnson Matthey*) onto the electrode support. All FTIR experiments were carried out using the same working electrode. Prior to each experiment, the supports of the electrodes were mechanically polished followed by a chemical cleaning in concentrated sodium hydroxide and nitric acid solutions, subsequently

* Electrochemical Society Student Member.
** Electrochemical Society Active Member.
z E-mail: ernesto@iqsc.usp.br

rinsed with ultra-pure water (Milli-Q, 18.2 MΩ cm). To activate the surface of the working electrode, the WE was cycled in H_2SO_4 solution from 0 to 1.75 V, at 0.2 V s^{-1} and then it was transferred protected by a droplet of electrolyte, in order to attach the aqueous suspension of the black platinum catalyst on the support. In order to compare the intrinsic activities in the different supporting electrolytes, the currents obtained for the ethanol electro-oxidation were normalized per total surface active area estimated by stripping a monolayer of CO, considering 420 μC cm^{-2} as the standard charge for desorbing a monolayer of CO on polycrystalline Pt. For this purpose, the CO saturation coverage on the catalysts was achieved by bubbling CO for 10 min at 0.05 V followed by bubbling Argon for 40 min in order to eliminate dissolved CO.

All experiments were performed at controlled temperature (23 ± 0.1 °C). The study was carried out with high purity reagents in the range from 0.01 to 1.0 mol L^{-1} ethanol (Merck) in either 0.5 mol L^{-1} sulfuric acid (Merck) or 0.1mol L^{-1}perchloric acid (Merck). All electrolyte solutions were prepared in ultra-pure water purified in a Milli-Q (18.2 MΩ cm) system and deaerated with Argon (4.8). The potential was held at 0.05 V vs. RHE and the mixture was homogenized by bubbling Argon for ca. 30 s after introducing the ethanol into the supporting electrolyte before starting the potentiostatic and potentiodynamic measurements. During the FTIR measurements the working electrode was downed. The potential scan was started immediately after homogenization of the mixture and waiting for the ethanol adsorption for ca. 120 s. All recorded spectra were collected during a potential step from 0.05 V to 1.0 V after the ethanol was added into the cell with the electrode polarized at 0.05 V vs. RHE.

Results and Discussion

Figure 1 depicts the typical voltammetric profile (cyclic voltammogram - CV) (a) of faradaic current density and (b) of the electro-oxidation of ethanol on unsupported Pt (J-M) nanoparticles in either $HClO_4$ (solid line) or H_2SO_4 (symbol line) electrolyte solutions.[28,29,37]

The definition of the peak and the symmetry of the adsorption states in Figure 1a are indicative of the surface cleanliness. These peaks occur due to the competition between the adsorption/desorption of molecular hydrogen, perchlorate anions (ClO_4^-) and (bi) sulfate anions (HSO_4^- or SO_4^{-2}) at Pt sites.[28,29,37] As it is well known, the CV profile of the commercial unsupported Pt (J-M) catalysts in acid electrolyte is more structured than that of carbon-supported Pt nanoparticles, which presents signatures such as symmetrical peaks at 0.12 V and 0.29 V, which correspond to (110)- and (100)-type step sites, respectively, and distinct features with a shoulder centered at 0.5 V, characteristic of small (111)-ordered surface domains.[28,29,37] In addition, a recent study[29] showed that commercial unsupported Pt (J-M) has larger agglomerated particles with crystalline size around 9 nm.[29] However, the CV profiles in Fig. 1a, do not suggest specific crystallographic orientation and can be considered as corresponding to a highly structured polycrystalline surface.

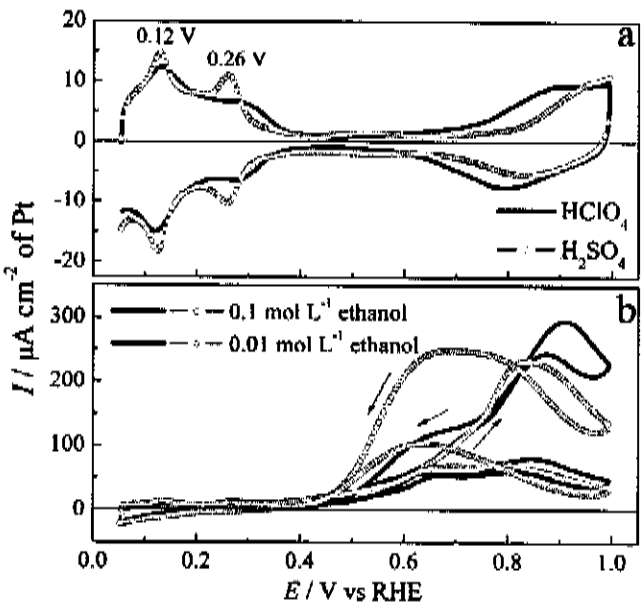

Figure 1. Cyclic voltammograms (a) of faradaic current density and (b) of the electro-oxidation of ethanol in either $HClO_4$ (solid line) or H_2SO_4 (symbol line) electrolyte solutions on unsupported Pt (J-M) nanoparticles. The cycles were recorded at 0.01V s^{-1} and 25 °C

Figure 1b presents only the first CVs in the ethanol concentrations 0.01 and 0.1 mol L^{-1}. The CVs profiles (only shown for 0.01 and 0.1 mol L^{-1} of ethanol) reveal that the onset of the oxidative current in the positive potential scan occurs at about 0.4 V vs. RHE, with one subtle shoulder at 0.7 V and a peak at 0.9 V. In the cathodic sweep occurs the reactivation of the reaction which appears as a shoulder between 0.6 and 0.7 V. In the subsequent voltammetric cycles, the surfaces are blocked by adsorbed intermediates, such as CO_{ad}, and CH_{ad}[9,16,18,19,26] formed in the preceding cathodic sweep and then the anodic peak is smaller because these adsorbed intermediates are only oxidized at high potentials.

In order to further explore the results presented in Figure 1 during the electro-oxidation of ethanol on unsupported Pt (J-M) catalysts in $HClO_4$ electrolyte, the formation of the adsorbed intermediates and reaction products were followed by in situ FTIR measurements in the different concentrations of ethanol (0.01 to 1.0 mol L^{-1}).

Figure 2 shows typical spectra during the electro-oxidation of ethanol on Pt (J-M) for alcohol concentrations of (a) 0.01 mol L^{-1}, (b) 0.1 mol L^{-1} and (c) 1.0 mol L^{-1} in potentiodynamic mode with the reference spectrum (Ro) measured at 0.05 V.

The bands due to the formation of soluble products on the electro-oxidation of ethanol, such as CO_2 (2343 cm^{-1})[6], acetic acid (1370 and 1280 cm^{-1})[6] and acetaldehyde (933 cm^{-1})[6] are identified. In addition, at 1400 cm^{-1} appears a band for all ethanol concentrations, which has been reported for bridging and bi-dentate acetate complexes from acetate species[32,33] or from acetic acid[18,34] at the Pt surface. Likewise, bands of C-O stretching modes for the formation of adsorbed carbon monoxide are observed at 2040 cm^{-1} (CO_{ad} – linear form) and at 1917 cm^{-1} (CO_B – bridge form). Bands at 2040 cm^{-1} of linearly adsorbed CO_{ad} are observed for all ethanol concentrations. Moreover, a subtle broad band at 1917 cm^{-1} from 0.3 to 1.0 mol L^{-1} ethanol is identified suggesting the formation of bridge adsorbed CO (CO_B) (Figure 2). But, the bridge CO band at Pt is given in the literature at 1850 cm^{-1}.[18] This shift may be due to a hybridization form between single and double bonds. In addition, the observation of bridge adsorbed CO at Pt sites has been observed in sulfuric acid only, and previous studies of ethanol electro-oxidation had reported the absence of bridge bond CO in $HClO_4$ electrolyte.[4,6,18,19] The presence of bridge CO on unsupported Pt agglomerates show that the structure to this material presents a different behavior in comparison with single and bulk platinum, which may be due to the larger amount of adsorbed intermediates at Pt surface.

During the electro-oxidation of ethanol to CO_2 occurs the dual pathway mechanism: (i) indirect pathway (*via* CO_{ad})[4,6,9,26] and at the same time (ii) direct pathway (*via* reactive intermediate).[7,26,18] In the case of the indirect pathway, the formation of adsorbed hydrocarbon fragments may occur (CH_{ad} with one or two carbons) which are oxidized to CO_2 at higher overpotentials.[9,16,18,19,26] In parallel, the electro-oxidation of ethanol may form acetic acid and acetaldehyde as end-products of the reaction.[9,22,25,26] Figure 3 shows qualitatively absorbance bands of CO_2 (square), CO_{ad} (circle), acetic acid (triangle) and acetaldehyde (star), normalized by their maximum absorbance for each species.

Behavior of CO_{ad} and CO_2.— The main aspect to be noted in Figure 3 is that the surface coverage of linearly adsorbed CO_{ad} at unsupported platinum nanoparticles increased with the concentration of

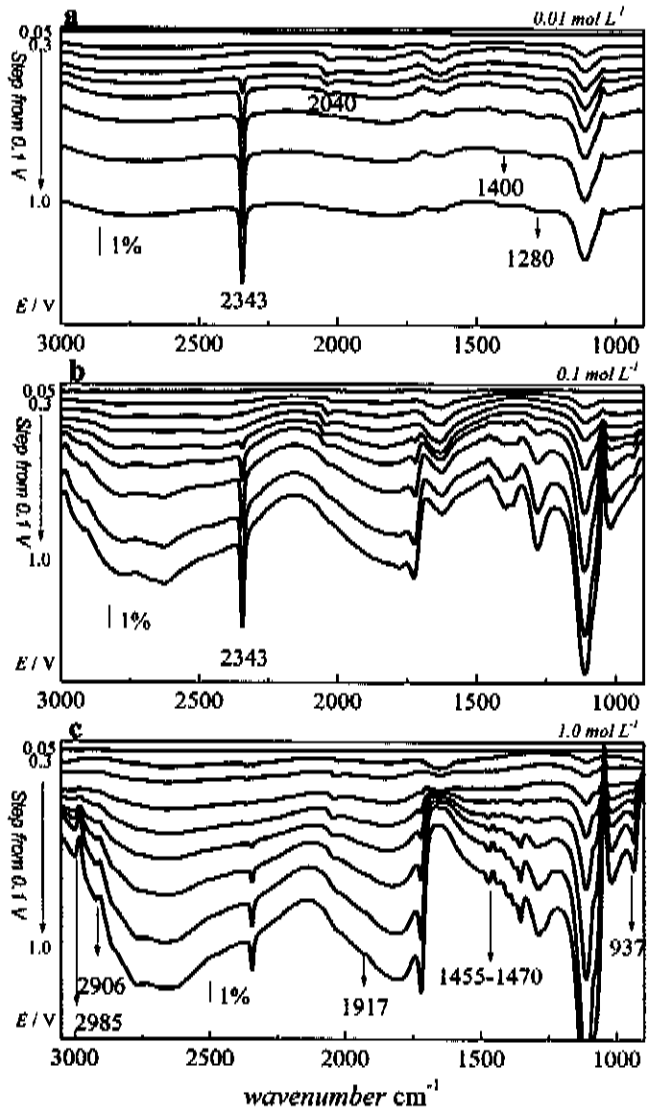

Figure 2. In situ FTIR spectra for ethanol electro-oxidation at Pt (J-M) agglomerates in 0.1 mol L^{-1} $HClO_4$. (a) 0.01 mol L^{-1}, (b) 0.1 mol L^{-1} and (c) 1.0 mol L^{-1} of ethanol. The spectra were obtained after potential steps from 0.05V. Ro = 0.05 V.

ethanol. However, the onset of the formation of adsorbed CO_{ad} occurs at 0.3 V for all ethanol concentrations, reaching a local maximum of intensity at 0.55 V. Immediately after the degree of coverage of adsorbed CO_{ad} reaches the maximum, the production of CO_2 occurs. Rapidly, at low concentration of ethanol (from 0.01 to 0.1 mol L^{-1}), the production of CO_2 reaches a maximum intensity around 0.8 V, which concurrently shows the decrease of the CO_{ad} band. Therefore, most formation of CO_2 occurred *via* CO_{ad} (indirect pathway), at least in this case of 0.01 mol L^{-1} of ethanol. Nevertheless, the CO_{ad} band is not totally suppressed at higher concentrations of ethanol (from 0.3 to 1.0 mol L^{-1}), because the coverage of adsorbed CO_{ad} is kept constant until higher overpotentials. In addition, a higher surface coverage by adsorbed CO_{ad} observed for potentials higher than 0.8 V was not reported in the literature yet. Possibly, this increase on the intensity of the band for adsorbed CO_{ad} occurs *via* a reactive intermediate as CH_3CHO_{ad} (direct pathway) at higher concentrations of ethanol.[18,26] So, in this case of higher concentrations of ethanol, the formation of CO_2 may follow a direct pathway mainly at high overpotentials. Furthermore, at low concentrations of ethanol, another important finding

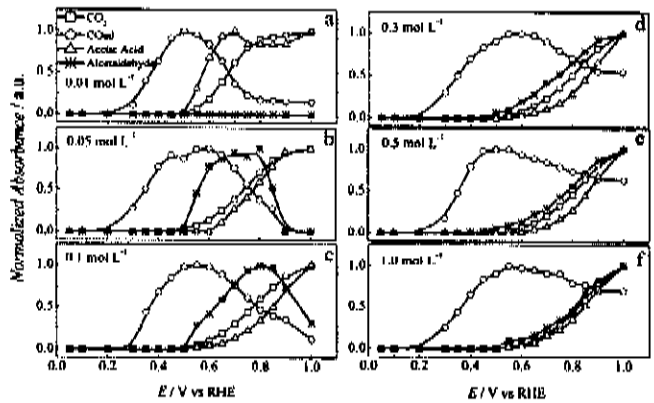

Figure 3. Normalized spectra of the CO_2 (square), CO_{ad} (cycle), acetic acid (triangle) and acetaldehyde (star) bands during ethanol electro-oxidation on the unsupported Pt (J-M) for all concentrations (a) 0.01 mol L^{-1}, (b) 0.05 mol L^{-1}, (c) 0.1 mol L^{-1}, (d) 0.3 mol L^{-1}, (e) 0.5 mol L^{-1} and (f) 1.0 mol L^{-1} of ethanol. The spectra were normalized by the maximum intensity absorbances for each species, respectively. Ro 0.05 V.

is that the intensity of the CO_2 band increases at potentials higher than 0.75 V, in which the CO_{ad} has been completely oxidized, decreasing the band to negligible intensities prior to 1.0 V. These observations reveal that at least part of the CO_2 is not coming from the indirect pathway at high potentials. Additionally, it suggests that the formation of CO_{ad} occurs *via* a reactive intermediate as CH_3CHO_{ad}, and that CO_{ad} is more stable at high overpotentials than at low overpotentials.

Finally, the formation of CO_2 can occur *via* the indirect pathway at low concentrations of ethanol or *via* the direct pathway at higher concentrations of ethanol. These may be the reasons for the different rates for formation of CO_{ad} and CO_2 at different concentrations of ethanol in Figure 3.

Behavior of acetic acid and acetaldehyde.— Figure 3 shows the formation of acetic acid and acetaldehyde during the electro-oxidation of ethanol. The onset of the acetaldehyde formation occurs at 0.55 V, and shows a subtle broad peak in the CO_{ad} profile at the same time mainly at 0.05 mol L^{-1} ethanol. This shoulder may be due to the CO_{ad} formation *via* reactive intermediate from CH_3CHO_{ad} species (direct pathway), as discussed above. Interestingly, the formation of the aldehyde band does not occur at 0.01 mol L^{-1} ethanol. In the case of low ethanol concentrations, at 0.01 mol L^{-1}, the acetaldehyde band shows a weak molar absorptivity due to the reduced formation.[35] So, in this concentration of ethanol, the formation of acetaldehyde cannot be completely excluded. Another interesting aspect in Figure 3a, at 0.01 mol L^{-1} of ethanol, is the fact that the formation of acetic acid occurs before the CO_2 formation. Previous works have reported that for ethanol electro-oxidation at Pt the formation of acetic acid occurs *via* acetaldehyde oxidized as an intermediate.[18,19,33] However, recent papers by Baltruschat group[26] and Giz and co-workers[7] showed that acetic acid may be formed by a parallel pathway. So, our data are in agreement with recent works,[7,26] which show a dual pathway for acetic acid formation at 0.01 mol L^{-1} of ethanol.

However, during the dual pathway in the acetic acid formation, it is not well-known the nature of the adsorbed intermediate and if it can occur at other concentrations of ethanol. In addition, for all other ethanol concentrations (0.05 to 1.0 mol L^{-1}) it is observed the increase of the intensity of the acetic acid band at high overpotentials, where the band for acetaldehyde reaches a maximum, showing that the formation of acetic acid occurs *via* acetaldehyde as intermediate (*via* acetate) at higher concentrations of ethanol.

Focusing now in the similar treatment of the bands given in Figure 3 the behavior of acetate species and acetic acid formation can be understood. Figure 4 shows the data for acetate species

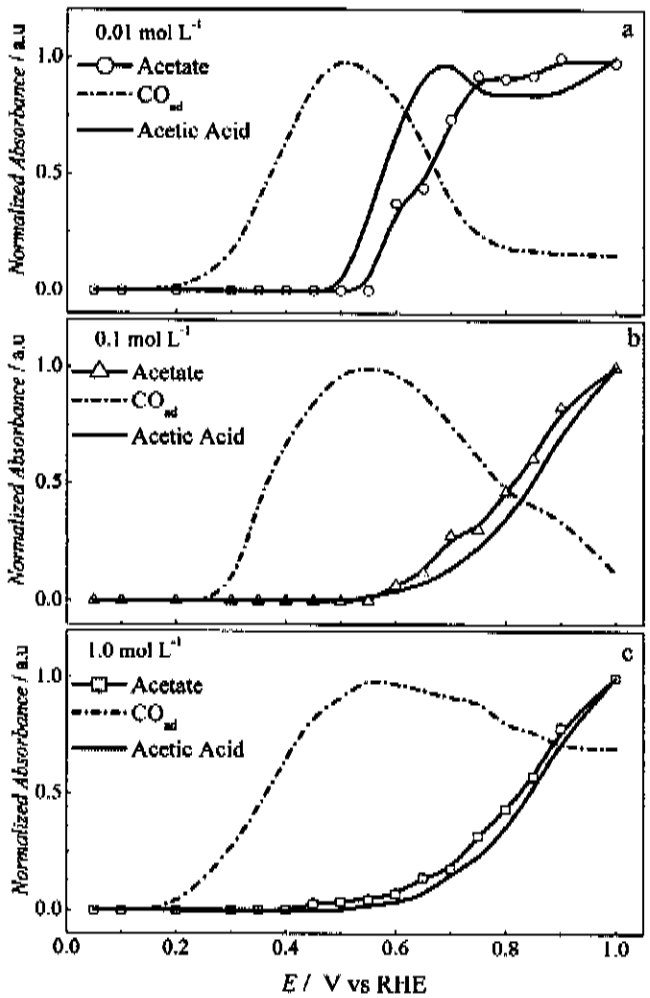

Figure 4. Normalized spectra during ethanol electro-oxidation catalyzed by unsupported Pt (J-M). Acetate (symbol line), CO_{ad} (dot line) and Acetic Acid (solid line) bands for ethanol concentrations of (a) 0.01 mol L^{-1}, (b) 0.1 mol L^{-1} and (C) 1.0 mol L^{-1}. The spectra were normalized by the maximum intensity absorbances for each species, respectively. Ro = 0.05 V.

(symbol line), CO_{ad} (dot line) and acetic acid (solid line) bands at 0.01 mol L^{-1} (a), 0.1 mol L^{-1} (b) and 1.0 mol L^{-1} (c) of ethanol.

Figure 4 shows that the shape of the band profile at 1400 cm^{-1} (acetate species) follows the behavior of the acetic acid band for ethanol concentrations of 0.05 until 1.0 mol L^{-1}. However, the acetic acid band does not follow the acetate species for ethanol concentration of 0.01 mol L^{-1}. Overall, therefore, the formation of acetic acid shows an influence of ethanol concentration. So, at 0.01 mol L^{-1} of ethanol, most acetic acid formation proceeds without the formation of adsorbed acetate intermediate between 0.5 and 0.70 V. However, at higher overpotentials, it is observed that the acetate band increases to a maximum intensity, showing that a parallel dual pathway occurs at 0.01 mol L^{-1} of ethanol. Additionally in Figure 4, for all other ethanol concentrations, the formation of acetic acid proceeds *via* adsorbed acetate species.

Mechanism proposed for ethanol electro-oxidation at unsupported Pt agglomerates. Effect of the ethanol concentration in the distribution of products.— There are mainly two possible forms proposed for ethanol adsorption on the Pt surface.[4,18,19,26] Similarly, we considered these possible forms of adsorption of the ethanol on unsupported Pt (J-M) agglomerates. As discussed in the literature[4], in the first

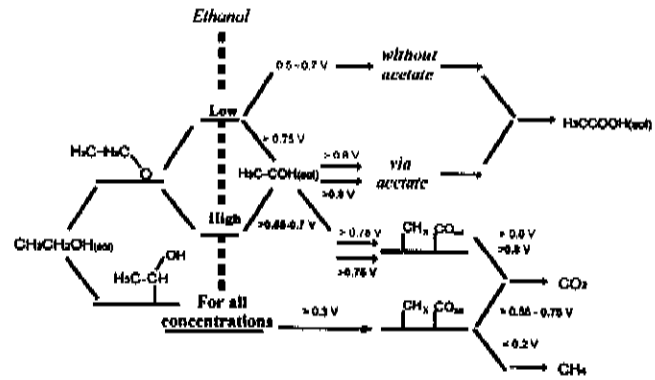

Scheme 1. Reaction mechanism during the electro-oxidation of ethanol on unsupported Pt (J-M) nanoparticles. The dual pathways correspond to the formation of CO_2 and acetic acid as end-products of the reaction. Each pathway is discussed in detail in the text.

model of adsorption, the ethanol is adsorbed by C1-species on surface. Moreover, the observation of the C-O stretch band for Pt-$COHCH_3$ species is not impossible because the dipole moment of the C-O bond has a small perpendicular component to the surface. Besides, the vibration of the ClO_4^- ions (1110 cm^{-1}) in this region may cover the C-O band at 1000–1050 cm^{-1}. It was, however, reasonable to assume the possibility of the existence of ethanol adsorbed from C1-species on the catalyst surface due to the observation of CO_{ad} fragments at low potentials (Figure 2c) and as given by previous work.[18,19] In the second model of adsorption, it was observed the ethoxi group, Pt-$OCHCH_3$ by in situ FTIR[4], suggesting the adsorption of the ethanol from the O-atom.

Considering all observations substantiated by our data and previous work,[4,18,19,26] a summary of the influence of all the adsorbed intermediates in the distribution of products of the reaction is presented in Scheme 1.

Conclusions

Selective pathways during the ethanol electro-oxidation on unsupported Pt catalysts showed a strong dependence with adsorbed intermediates under different ethanol concentrations. Our data showed that at low ethanol concentrations (0.01 to 0.05 mol L^{-1}) the reaction takes place mainly by CO_2 and acetic acid formation. In this conditions, most of the CO_2 formed *via* CO_{ad}. However, at low ethanol concentration and at overpotentials higher than 0.8 V at least part of the CO_2 is formed through the CH_3CHO_{ad} species (direct pathway). At higher concentrations of ethanol, however, most of CO_2 was formed *via* a reactive intermediate such as acetaldehyde (direct pathway). Nevertheless, the formation of acetic acid occurred *via* a dual pathway. Our data showed that the formation of acetic acid proceeded without the participation of acetate species only at 0.01 mol L^{-1} of ethanol at low overpotentials. However, the increase of the adsorbed intermediate CO_{ad} at Pt surface drives the reaction on a pathway via adsorbed intermediate as acetate species.

Acknowledgments

Financial support from CAPES, CNPq, and FAPESP, Brazil, is gratefully acknowledged. D.A. Cantane acknowledges a scholarship from CNPq.

References

1. W. Vielstich, H. Yokokawa, and H. A. Gasteiger, *Handbook of fuel cells: fundamentals, technology, and applications. Advances in electrocatalysis, materials, diagnostics and durability, part 1*, Wiley (2009)
2. K. Kordesch and G. Simader, *Fuel cells and their applications*, VCH, Weinheim (1996).

3. C. Lamy, A. Lima, V. LeRhun, F. Delime, C. Coutanceau, and J. M. Léger, *J. Power Sources*, **105**, 283 (2002).
4. T. Iwasita and E. Pastor, *Electrochim. Acta*, **39**, 531 (1994).
5. F. Colmati, G. Tremiliosi-Filho, E. R. Gonzalez, A. Berná, E. Herrero, and J. M. Feliu, *Phys. Chem. Chem. Phys.*, **11**, 9114 (2009).
6. G. Camara and T. Iwasita, *J. Electroanal. Chem.*, **578**, 315 (2005).
7. M. Ciz and G. Camara, *J. Electroanal. Chem.*, **625**, 117 (2009).
8. H. Hitmi, E. M. Belgsir, J-M. Léger, C. Lamy, and R. O. Lenza, *Electrochim. Acta*, **39**(3), 407 (1994).
9. H. Wang, Z. Jusys, and R. Behm, *J. Phys. Chem. B*, **108**, 19413 (2004).
10. J. P. I. Souza, S. L. Queiroz, and F. C. Nart, *Quím. Nova*, **23**, 384 (2000).
11. H. Wang, Z. Jusys, and R. Behm, *J. Power Sources*, **154**, 351 (2006).
12. T. Iwasita, B. Rasch, E. Cattaneo, and W. Vielstich, *Electrochim. Acta*, **34**, 1073 (1989).
13. S. C. Chang, L. W. H. Leung, and M. J. Weaver, *J. Phys. Chem.*, **94**, 6013 (1990).
14. T. Iwasita and F. Nart, *Prog. Surf. Sci.*, **55**, 271 (1997).
15. G. Camara, R. De Lima, and T. Iwasita, *Electrochem. Commun.*, **6**, 812 (2004).
16. S. C. S. Lai and M. T. M. Koper, *Faraday Discuss.*, **140**, 399 (2008).
17. S. C. S. Lai and M. T. M. Koper, *J. Phys. Chem. Lett.*, **1**, 1122 (2010).
18. R. B. Kutz, B. Braunschweig, P. Mukherjee, R. L. Behrens, D. D. Dlott, and A. Wieckowski, *J. Catal.*, **278**, 181 (2011).
19. S. C. S. Lai, S. E. F. Kleyn, V. Rosca, and M. T. M. Koper, *J. Phys. Chem. C*, **112**, 19080 (2008).
20. A. Lagutchev, G. Q. Lu, T. Takeshita, D. D. Dlott, and A. Wieckowski, *J. Chem. Phys.*, **125**, 154705 (2006).
21. G. Tremiliosi-Filho, E. Gonzalez, A. Motheo, E. Belgsir, J. M. Léger, and C. Lamy, *J. Electroanal. Chem.*, **444**, 31 (1998).
22. D. A. Cantane and E. R. Gonzalez, *ECS Transactions*, **25**, 1161 (2009).
23. F. Lima and E. Gonzalez, *Electrochim. Acta*, **53**, 2963 (2008).
24. F. Lima, D. Profeti, W. Lizcano-Valbuena, E. Ticianelli, and E. Gonzalez, *J. Electroanal. Chem.*, **617**, 121 (2008).
25. U. Schmiemann, U. Muller, and H. Baltruschat, *Electrochim. Acta*, **40**, 99 (1995).
26. A. A. Abd-El-Latif, E. Mostafa, S. Huxter, G. Attard, and H. Baltruschat, *Electrochim. Acta* **55**, 7951 (2010).
27. H. S. Wang, C. Wingender, H. Baltruschat, M. Lopez, and M. T. Reetz, *J. Electroanal Chem.*, **509** 163 (2001).
28. J. Solla-Gullón, P. Rodriguez, E. Herrero, A. Aldaz, and J. M. Feliu, *Phys. Chem. Chem. Phys.*, **10**, 1359 (2008).
29. E. G. Ciapina, S. F. Santos, and E. R. Gonzalez, *J. Electroanal Chem.*, **644**, 132 (2010).
30. H. H. Wang, Z. Y. Zhou, Q. Yuan, N. Tian, and S. G. Sun, *Chem. Commun.*, **47**, 3407 (2011).
31. J. C. Bauer, X. Chen, Q. Liu, T. H. Phan, and R. E. Schaak, *J. Mater. Chem.*, **18**, 275 (2007).
32. A. Rodes, E. Pastor, and T. Iwasita, *J. Electroanal Chem.*, **376**, 109 (1994).
33. M. Heinen, Z. Jusys, and R. J. Behm, *J. Phys. Chem. C*, **114**, 9850 (2010).
34. A. Wieckowski, J. Sobkowski, P. Zelenay, and K. Franaszczuk, *Electrochim. Acta*, **26**, 1111 (1981).
35. P. Gao, S. C. Chang, Z. Zhou, and M. J. Weaver, *J. Electroanal. Chem.*, **272**, 161 (1989).
36. G. Socrates, *Infrared Characteristic Group Frequencies*; John Wiley & Sons: Chichester, (1980).
37. J. Solla-Gullon, F. Vidal-Iglesias, E. Herrero, J. Feliu, and A. Aldaz, *Electrochem. Commun.*, **8**, 189 (2006).